

**DETC2007-35712**

**MODELLING OF VISCOUS SQUEEZE-FILM DAMPING AND THE EDGE CORRECTION FOR  
PERFORATED MICROSTRUCTURES HAVING A SPECIAL PATTERN OF HOLES**

**Dorel Homentcovschi<sup>a)</sup>, Weili Cui and Ronald N. Miles**  
Department of Mechanical Engineering, State University of  
New York at Binghamton  
Binghamton, NY 13902-6000

<sup>a)</sup>Permanent address: *Politehnica* University of Bucharest,  
Applied Science Department  
E-mail: [homentco@binghamton.edu](mailto:homentco@binghamton.edu)

**Abstract**

This paper contains an analysis of the squeeze-film damping in micro-electromechanical devices having a planar microstructure containing a repetitive pattern of oval holes. The planar microstructures containing oval holes assure a better protection against dust particles and water drops than the microstructures having circular holes. Consequently, they should be preferred in designing protective surfaces for microphones working in natural environment.

Analytical formulas are provided for designing a planar microstructure with a periodic system of staggered holes to create a structure having minimum squeeze-

film damping with an assigned open area.

For the planar microstructures containing aligned oval holes an edge correction is given which accounts for the finite size of real structures.

**INTRODUCTION**

The sensing mechanism of many micro-electromechanical systems (MEMS) (such as microphones and microaccelerometers) is based on the capacitive detection principle. Many of these devices consist of parallel plate capacitors having a moving electrode (a diaphragm or proof mass) and a backplate. The small space between these elements is filled with fluid (air).

In some devices, in order to protect the diaphragm from external damage (for microphones working in natural environment) a certain perforated planar microstructure may be placed in the front of the microphone at a small distance from the diaphragm. In some design solutions a single perforated plate is used for both functions.

When the diaphragm is vibrating in the normal direction, the air film develops a pressure disturbance which opposes its motion (viscous air-gap mechanical resistance or squeeze-film damping.) In order to decrease the squeeze-film damping effect the backplate is often fabricated in the form of a perforated plate containing a periodic system of holes. MEMS also typically need etch holes to reduce the time required to release the micromechanical structure during the final release etch. A simplified model of the air motion for the case of circular holes has been considered by Škvor in [1]. He succeeded in obtaining a simple and useful formula for the total pressure which has been widely used for designing microphones.

Most applications employ only circular or square holes [2], [3]. The numerical simulation in this case is simple and for many MEMS gives the desired data for design purposes. Our analysis has revealed that other geometrical shapes of holes such as ovals are also suitable for decreasing the squeeze-film damping on the planar microstructures. As elongated ovals assure a better protection against dust particles and water drops (assumed generally as quasispherical) than the circular holes, in this paper we shall focus on the study of viscous damping for a repetitive pattern of oval holes. This type of geometry needs a more elaborate analysis of the viscous damping than that required for the circular holes.

The squeeze-film of air in a planar microstructure can be analyzed considering the Reynold's equation in a domain containing a periodic system of holes. Section 3 contains results of a numerical simulation of the squeeze-film viscous damping of a microstructure containing a staggered (off-set) system of oval holes. In presenting the results we show how to redesign a given planar microstructure having as its basic pat-

tern uniform spaced staggered circles into a planar microstructure based on oval holes with smaller squeeze-film damping for the same open area. The design parameters of the "initial microstructure" (containing circular holes) can be determined analytically and analytical formulas are provided for designing the "final" microstructure involving oval holes. The analytical formulas are based on the fitting of the data resulting from numerical simulations. The subsection including the designing formulas can be read independently of the other sections and the paper gives an example showing how the method works.

In Section 4 a simple method accounting for the finiteness of the real plates in the case of microstructures having aligned oval holes is presented. The opened edge correction consists of increasing the area of the edge cells until their total pressure equals the total pressure of an inner cell. An example of application of the edge correction is provided.

Besides the squeezed-film damping, the length of the holes equal to the thickness of the plate gives a supplementary damping due to the resistance of the holes. The analysis presented in this paper neglects the holes' resistance. Therefore, it can be directly applied in the case of thin plates. Also, the procedure developed for computing the squeeze film damping can be used in an integrated scheme for determining the total damping of the microstructure [4].

## THE PRESSURE EQUATION

### Stating of the problem

We consider an infinite plane plate having a system of holes which is invariant under the transformations of the group consisting of reflections, in two orthogonal lines, and translations by vectors which are multiples of the vectors  $\mathbf{c}_1$  and  $\mathbf{c}_2$  as shown in (Fig.1a). We isolate the *basic domain*  $D$ , which, when acted on by the transformations of the group can cover the whole plate. We assume that the holes are of oval form. By oval we mean a rectangle with two half-circles added to two opposite sides. As a particular structure we have also the circular holes case.

Micromechanical dynamics of the perpendicularly



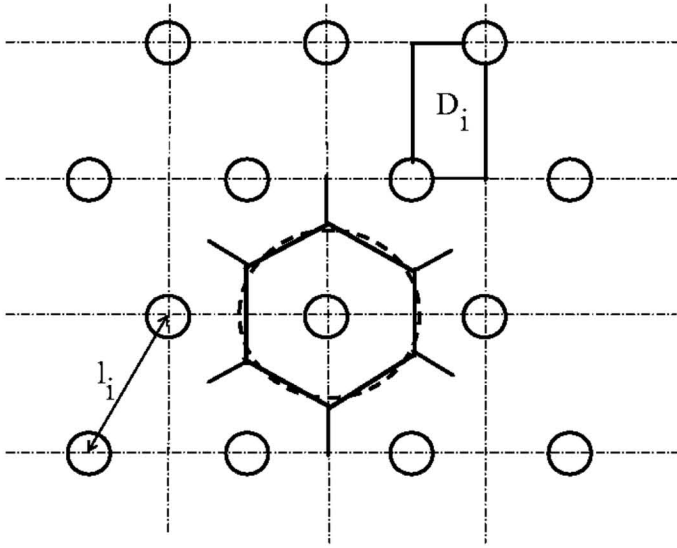


Fig. 2a The hexagonal influence domain of a hole, its equivalent circle and the basic domain  $D_i$

where the pressure coefficient  $C_p$  is

$$C_p = -2 \iint_{D'} p(x, y) dx dy \quad (8)$$

The canonical domain  $D'$  results from the basic domain  $D$  by the scaling relationship as shown in (Fig. 1b).

### SIMULATION OF THE SQUEEZE-FILM DAMPING IN THE CASE OF STAGGERED HOLES

#### Basic relationships

The design of the backplate for capacitive microphones is typically obtained by means of Skvors' formula [1]. Thus, for the system of off-set uniform spaced circular holes of  $r_i$ -radius in Fig. 2a the hexagonal influence region of a hole is approximated by a circle of  $0.525 l_i$  radius,  $l_i$  being the distance between the centers of two neighboring circles, having the same area.

A more precise calculation of the damping of the system of staggered circles can be obtained by solving the boundary-value problem (4), (5), (6) for the canonical domain  $D'_i$  in Fig.2b. The force  $F^{(i)}$  on a unit area of the initial system is given by (we consider  $L_0 = l_i$  for the initial structure)

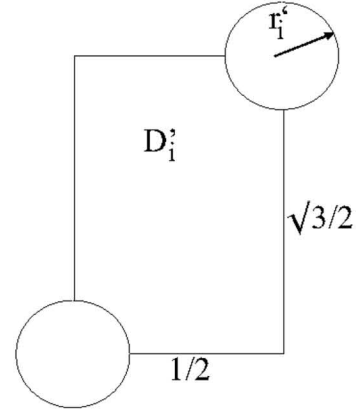


Fig. 2b The canonical domain corresponding to the domain in Fig. 2a

$$F^{(i)} = N^{(i)} F_i = \frac{12\mu}{d_0^3} N^{(i)} l_i^4 C_p^{(i)} w$$

where  $N^{(i)}$  is the number of circles (holes) on a unit area  $u^2$

$$N^{(i)} = \frac{2}{\sqrt{3} l_i^2} u^2 \quad (9)$$

and  $C_p^{(i)}$  is the pressure coefficient given by formula (8). The radii of the circular arcs in the canonical domain  $D'_i$  are  $r'_i$  and we have

$$r'_i = \frac{r_i}{l_i} \quad (10)$$

To obtain a device with a smaller viscous damping we consider the canonical domain  $D'_f$  in Fig.3a and the holes pattern resulting from this basic domain by symmetries with respect to coordinate axis, translations and similarity transformations Fig.3b. The holes have now an oval form and we denote by  $l_f$  the distance between the centers of two neighboring ovals (taken also as reference length for the final structure). The number of holes on a unit area  $u^2$  of the final structure  $N^{(f)}$  is

$$N^{(f)} = \frac{2}{\sqrt{3} l_f^2} u^2 \quad (11)$$

and, correspondingly, the force  $F^{(f)}$  (on a unit area) has the form

$$F^{(f)} = N^{(f)} F_f = \frac{12\mu}{d_0^3} N^{(f)} l_f^4 C_p^{(f)} w$$

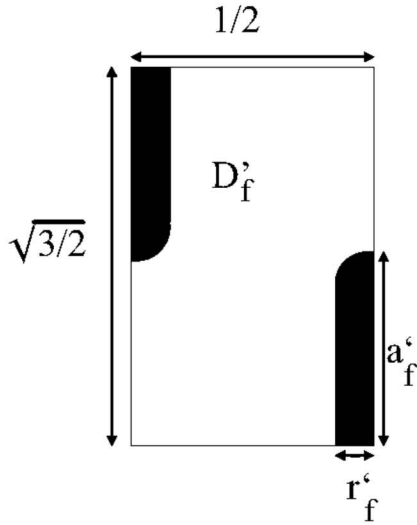


Fig.3a The canonical domain  $D'_f$

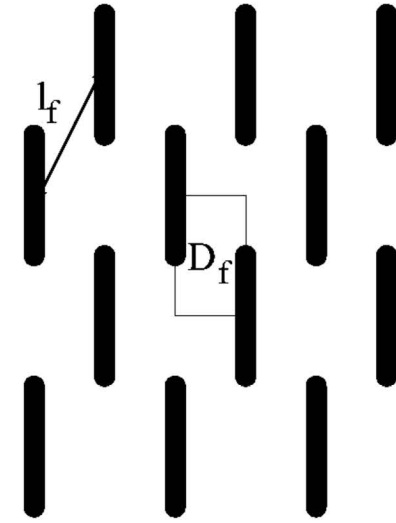


Fig. 3b The final structure

The radius of the circular arcs in domain  $D'_f$  is  $r'_f = r_f / l_f$ ; the condition that the two structures have the same *area ratio*  $AR$  yields

$$r'_f = \sqrt{\frac{\sqrt{3}AR}{2\pi}} \quad (12)$$

$$r'_f = \frac{\sqrt{3}AR}{4a'_f + \sqrt{16a'^2_f - (8 - 2\pi)\sqrt{3}AR}} \quad (13)$$

Finally, the ratio of the holes density in the two systems is

$$\frac{N^{(f)}}{N^{(i)}} = \frac{l_i^2}{l_f^2}$$

Hence

$$r_f = l_f r'_f \quad (14)$$

$$\frac{F^{(f)}}{F^{(i)}} = \frac{N^{(i)}}{N^{(f)}} \frac{C_p^{(f)}}{C_p^{(i)}} \quad (15)$$

Once the initial geometry ( $r_i$  and  $l_i$ ) is given and the ratio of the holes densities is specified, the relations (10-14) give the geometry of the oval ( $r_f$  and  $l_f$ ). The total pressure on the final structure is determined by relation (15) in terms of pressure coefficients and the total pressure on a unit area of the initial system.

#### Determination of the pressure coefficients

For obtaining the pressure coefficients  $C_p^{(i)}, C_p^{(f)}$  we use formula (8) which requires the preliminary determination of the functions  $p^{(i)}(x, y), p^{(f)}(x, y)$  solutions of the boundary-value problem (4) (5) (6) for the domains  $D'_i, D'_f$ , respectively. Since we will use these coefficients for designing purposes, these problems have to be solved many times. This is why we decided to consider a computationally efficient Boundary Element Method simulation which provides the values of the function and of its normal derivative along the boundary. Once these quantities are determined the total pressure upon the canonical domain can be also obtained analytically.

The ratio of the pressure coefficients  $C_p^{(i)}/C_p^{(f)}$  obtained by numerical simulation is plotted in Fig.4 versus area ratio  $AR$  for the cases:  $a/a_1 = 0.6 : 0.1 : 0.9$  (asterisks). Further analysis reveals that the ratio of the pressure coefficients can be fitted well by a third order polynomial:

$$\frac{C_p^{(f)}}{C_p^{(i)}} = e_3^i AR^3 + e_2^i AR^2 + e_1^i AR + e_0^i,$$

where the coefficients  $e_j^i$  are given in Table 1. Also, we have plotted in Fig.4 the least squares fitting by a cubic

$a_i^* \downarrow j \rightarrow$	3	2	1	0
0.6	3.4	-1.8	2.1	0.25
0.7	7.6	-4.6	2.3	0.15
0.8	4.9	-3.6	1.8	0.12
0.9	1.1	-1.5	1.3	0.12

Table 1. The coefficients  $e_j^i$  for  $a_i^* = a/a_1$  and  $j$

polynomial of the computed values for the ratio of the pressure coefficients (continuous line).

#### The design relationships and example of application

We summarize now the formulas for designing a plane microstructure based on an oval pattern of holes. In order to show how these formulas may be applied we consider also an example.

- Preliminary data

$\mu = 1.8 \cdot 10^{-5} N \cdot s/m^2$  the viscosity of the air

$d_0 = 0.005 mm$  the width of the air gap at equilibrium position (the nominal air-gap size)

$AR = 0.2$  the surface fraction occupied by the holes (the area ratio)

- Design parameters for the case of circular holes

$N^{(c)} = 250$  the number of the circular holes/ $mm^2$

- Determine

$r_i$ —the radius of circular holes

$$r_i = \sqrt{\frac{AR}{\pi N^{(c)}}} u$$

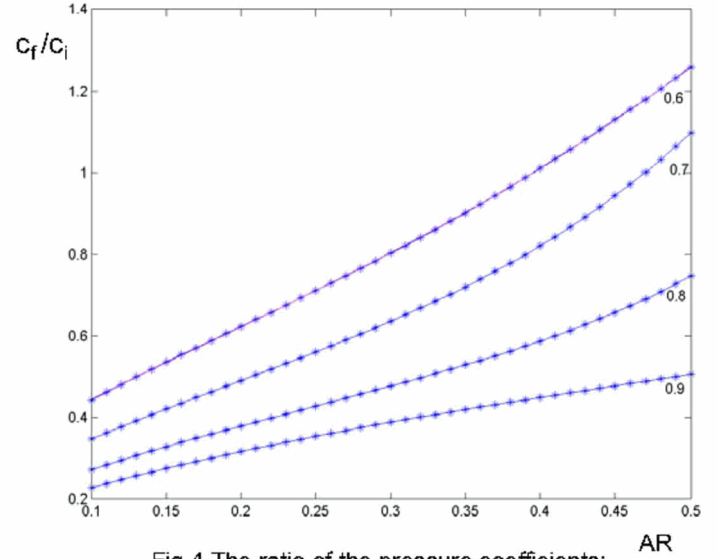


Fig.4 The ratio of the pressure coefficients: numerical simulation (\*) and fitted cubic (continuous line)

$l_i$ —the distance between two neighboring holes resulting from (9)

$$l_i = \frac{\sqrt{2}}{\sqrt[4]{3}} \frac{1}{\sqrt{N^{(c)}}} u$$

$F^{(c)}$ —the force/unit area (Improved Skvor's formula [6])

$$F^{(c)}/w = N^{(c)} \frac{12\pi\mu (0.525l_i)^4}{d_0^3} \left[ \frac{1}{2}AR - \frac{1}{4} \ln(AR) - \frac{1}{8}AR^2 - \frac{3}{8} + 10^{-4} \times (8.7 - 10AR + 26AR^2 - 23AR^3) \right]$$

In the considered example:  $r_i = 0.016 mm$ ,  $l_i = 0.068 mm$ ,  $F^{(c)}/w = 0.27 \times 10^{-3} Ns/m$ .

- Design parameters in the case of oval holes

$N^{(f)}$ —the number of the oval holes/ $mm^2$

As application we consider two cases:  $N_1^{(f)} = 250$  and  $N_2^{(f)} = 500$ .

- Determine final force on a *unit area* (15) as

$$F_j^{(f)} = \frac{C_p^f N^{(i)}}{C_p^i N^{(f)}} F^{(i)},$$

We take also  $k_1 \equiv a/a_1 = 0.9$  for the first case and  $k_2 \equiv a/a_1 = 0.8$  in the case  $N_2^{(f)} = 500$ . There results

$$F_1^{(f)}/w = 0.9 \times 10^{-4} N \text{ s/m} \text{ and } F_2^{(f)}/w = 0.5 \times 10^{-4} N \text{ s/m}$$

- Determine the geometrical dimensions of the basic cell and oval holes

$l_f$ —the *distance between the centers of two neighboring ovals* from (11) as  $l_f = a_{1f}, b_{1f}$ —the *basic cell dimensions*

$$a_{1f} = \frac{\sqrt{3}}{2} l_f; \quad b_{1f} = \frac{1}{2} l_f$$

$r_f$ —the *radius of the half circles at the oval ends* (or the *half-width of the oval rectangle*)

$$r_f = \frac{\sqrt{3} l_f^2 AR}{4a_f + \sqrt{16a_f^2 - (8 - 2\pi) \sqrt{3} l_f^2 AR}}$$

In the considered examples we obtain:

$$l_{f1} = 0.068mm, a_{1f1} = 0.059mm, b_{1f1} = 0.034mm, a_{f1} = 0.053mm, r_f = 0.0038mm.$$

$$l_{f2} = 0.048mm, a_{1f2} = 0.038mm, b_{1f1} = 0.024mm, a_{f1} = 0.034mm, r_f = 0.003mm.$$

**Remark 1** *When the air gap is small the continuum behavior of the gas breaks down. In this case, gas rarefaction should be taken into account in the model. The Reynolds equation (1) is still valid if the viscosity coefficient  $\mu$  is substituted by*

$$\mu_{eff} = \frac{\mu}{1 + 6.096 \lambda' / d_0}$$

where the mean free path  $\lambda' = 0.0068/p^a$  at ambient temperature and pressure  $p^a$  [7].

## THE CASE OF OVAL ALIGNED HOLES: THE EDGE CORRECTION

The analysis in the previous sections has assumed an infinite planar microstructure. The real structures are bounded having several edges. The homogeneous Neumann boundary condition (6) imposed on a closed side of the domain is compatible with the condition on the external curve of the cell. Consequently, the closed edges of the microstructure don't need any correction. On the other side the boundary condition  $p = 0$ , fulfilled along an open edge, is different from the homogeneous Neumann condition required by the cell's external curve. The new boundary condition makes the total pressure for an edge cell to be smaller than that corresponding to a regular (inner) cell. This gives a pressure change from cell to cell which destroys the periodicity of the solution and makes the calculations more complicated.

In the case of circular aligned holes a method was given in [8] for introducing an edge correction. Thus, for an edge cell the sides of the cell perpendicular to the edge are increased with a certain length  $dd$ . By a proper choice of this length it is possible to increase the total pressure of an edge cell to the value of an inner cell. Numerical simulations have proved that this correction works well and the periodicity of pressure being re-established (with a certain approximation) for all the inner cells.

In the case of aligned oval holes the situation is different. Accounting for the relative position of the hole with respect to the edge line two corrections can be determined. Thus the correction  $dd_1$  corresponds to the case where the oval hole is parallel to the  $Ox$ -direction and the correction  $dd_2$  results in the case where the oval hole is parallel to the direction  $Oy$ . Generally,  $dd_1 \neq dd_2$  and the value of the correction to be used for a certain edge side depends on its orientation. To show how the edge correction works in the case of a perforated planar structure having aligned oval holes consider as the basic canonical domain the rectangle in Fig.5 denoted by  $D_{SE}$ . In the numerical calculations  $d_1 = \sqrt{3}$ ,  $d_2 = 1$ ,  $r' = 0.1$ ,  $a' = 0.45$  were chosen. Inside the domain  $D_{SE}$  the pressure satisfies equation

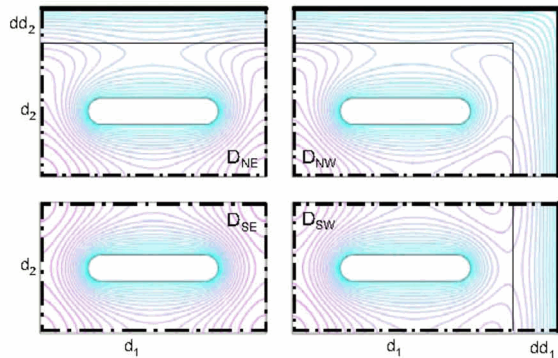


Fig.5 The inner cell and the edge cells in the case of aligned oval holes

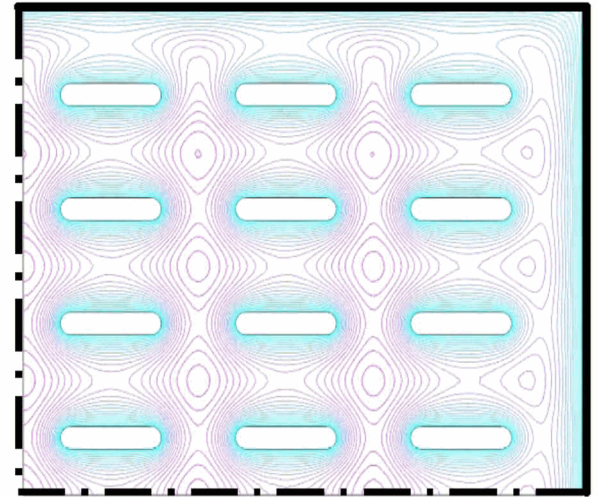


Fig.6 A finite perforated microstructure containing aligned holes

(4) and along the boundaries the conditions (5) and (6). The level lines of the pressure are plotted in the domain  $D_{SE}$ . The total pressure for the canonical domain is  $P_{SE} = 0.155625$ .

In the case of the domain  $D_{SW}$  the right-hand side is supposed to be an open boundary (continuous line). Correspondingly the zero pressure condition stands for the zero flux condition along this side

$$p = 0, \text{ along the inner boundary } \cup \text{ right-hand side}$$

$$\frac{\partial p}{\partial n} = 0, \text{ along the remaining boundary of the cell}$$

and the resulting total pressure is  $P_{SW} = 0.109702$ . By increasing the lengths of the upper and lower sides of the cell by  $dd_1 = 0.334$  the total pressure is increasing until value  $P_{SW} = 0.156771$  (the relative error is  $|P_{SE} - P_{SW}|/P_{SE} = 0.6\%$ ). The level lines of the pressure in this last case are plotted also in the domain  $D_{SV}$ .

Similarly, for the domain  $D_{NE}$  the upper side is an open boundary side. The initial total pressure is  $P_{NE}^* = 0.093319$ . By increasing the length of the vertical sides by  $dd_2 = 0.3$  there results  $P_{NE} = 0.154206$  the relative error (as compared with an inner cell) being 0.9%.

The domain  $D_{NW}$  has the upper and right-hand sides as boundary opened sides. Thus, this cell is considered as a corner cell. Their dimensions result as being  $d_1 + dd_1$  and  $d_2 + dd_2$ . The level lines of the pressure are plotted in the domain  $D_{NW}$  and the total pressure is  $P_{NW} = 0.15972$ . The relative error as compared with the inner cell  $D_{SW}$  is 2.6%.

Let us consider now the perforated planar microstructure in Fig.6 containing 12 oval holes and having the upper and right-hand side external lines opened and the left-hand side and lower external lines closed. The inner canonical cell has the same dimensions as before and the corrections  $dd_1$  and  $dd_2$  were applied to the vertical and horizontal edge cells, respectively. The figure includes the pressure level lines obtained by using a FEM software. It is clear that the periodicity of the pressure holds for the inner cells. The total pressure of the structure obtained by using the FEM software is  $PT = 1.872$ . On the other hand let us denote  $PT_1 = 12 * P_{SE}$ . Then  $PT_1 = 1.8675$  and there results

$$PT_{error} = \frac{|PT - PT_1|}{PT} = 2.4\%$$

The dimensions of the corrected corner cell are completely determined by the corrections of the two sides meeting at the corner point. Consequently, the only way to improve the precision of approximation (under 2.4%) is to modify the dimensions of the corner holes.

The presented method is useful in the case of domains containing hundreds of holes especially when the holes' resistance has to be taken into account.

**Remark 2** *Other approaches for taking into account the real geometry of a perforated microstructure were considered by Veijola and Matilla [9] and by Bao et al. [10]. They add an additional "leakage" term, due to perforations, to the classical Reynolds' equation. The resulting equation (the "modified Reynolds' equation") has to be integrated by using a numerical method for every specified structure. The advantage of our approach of the edge correction is evident: we have to modify only the dimensions of the open side cells.*

## CONCLUSIONS

The main accomplishments of this work are:

- Analysis of perforated planar microstructures containing a repetitive pattern of oval staggered holes.
- Provides analytical formulas for redesigning a periodic perforated planar microstructure containing circular holes into a structure with a lower squeeze-film damping based on a repetitive pattern of staggered oval holes of the same open area.
- Introduction of an edge correction for the perforated planar microstructures containing an aligned system of oval holes.
- The use of the staggered holes permits a better use of material, resulting in a smaller total pressure for a given amount of open area. However, in the case of staggered holes, we do not know a simple method to take into consideration the effects of the finiteness of the microstructure.

## ACKNOWLEDGEMENTS

This work has been supported through NIH grant R01 DC05762-1A1 to RNM

## References

1. Škvor, Z., *On acoustical resistance due to viscous losses in the air gap of electrostatic transducers*, *Acustica*, Vol. **19**, (1967-1968), pp. 295-297.
2. Starr, J.B., *Squeeze-film damping in solid-state accelerometers*, Tech. Digest IEEE Solid State Sensor and Actuator Workshop, Hilton Head Island SC, June 1990, pp.44-47.
3. Nayfeh, A.H. and Younis, M.I., *A new approach to the modeling and simulation of flexible microstructures under the effect of squeeze-film damping*, *J. Micromech. Microeng.*, vol. **14**, (2004), pp. 170-181.
4. Homentcovschi, D. and Miles, R. N., *Modelling of viscous damping of perforated planar micromechanical structures. Applications in acoustics*, *J. Acoust. Soc. Am.*, Vol. **116**, No. 5, (2004), pp.2939-2947.
5. White, F.M., *Viscous fluid flow*, Mc.Graw, 1991
6. Homentcovschi, D. and Miles, R. N., *Viscous Damping of Perforated Planar Micromechanical Structures*, *Sensors and Actuators*, Vol. A 119, (2005), pp. 544-552.
7. Ebert, W.A., and Sparrow, E.M. *Slip flow in rectangular and annular ducts*. *J. Basic Eng. Trans. ASME* Vol.**87**, (1965), pp.1018–1024.
8. Homentcovschi, D. and Miles, R. N., *Viscous microstructural dampers with aligned holes: design procedure including the edge correction*. To appear in *Journal of the Acoustical Society of America*.
9. Veijola, T., Mattila, T., *Compact squeezed-film damping model for perforated surface*, *Proc. Transducers '01*, München, Germany, June 10-14, 2001, pp.1506-1509.
10. Bao, M., Yang, H., Sun, Y., French, P.J., *Modified Reynolds' equation and analytical analysis of squeeze-film air damping of perforated structures*, *J. Micromech. Microeng.*, Vol. **13** (2003), pp. 795-800.